Non-Markovian dynamics of a single electron spin coupled to a nuclear spin bath

E. Ferraro,[1,*] H.-P. Breuer,[2,3,†] A. Napoli,[1] M. A. Jivulescu,[1] and A. Messina[1]

[1]*Dipartimento di Scienze Fisiche ed Astronomiche, Università di Palermo, via Archirafi 36, 90123 Palermo, Italy*
[2]*Physikalisches Institut, Universität Freiburg, Hermann-Herder-Strasse 3, D-79104 Freiburg, Germany*
[3]*Hanse Wissenschaftskolleg, Institute for Advanced Study, D-27733 Delmenhorst, Germany*

We apply the time-convolutionless (TCL) projection operator technique to the model of a central spin, which is coupled to a spin bath via nonuniform Heisenberg interaction. The second-order results of the TCL method for the coherences and populations of the central spin are determined analytically and compared to numerical simulations of the full von Neumann equation of the total system. The TCL approach is found to yield an excellent approximation in the strong field regime for the description of both the short-time dynamics and the long time behavior.

I. INTRODUCTION

Projection operator techniques[1] are widely used in studies of the dynamical behavior of complex open quantum systems featuring non-Markovian relaxation and decoherence phenomena.[2] The most prominent variant of these techniques is the Nakajima-Zwanzig (NZ) projection operator method, which leads to an integrodifferential equation for the reduced density matrix of the open system containing a certain memory kernel.[3,4] An alternative and technically much simpler scheme is the time-convolutionless (TCL) projection operator technique in which one obtains a first-order differential equation for the reduced density matrix.[5] The advantage of the TCL approach consists in the fact that it yields an equation of motion for the relevant degrees of freedom, which is local in time and therefore often much easier to deal with than the NZ master equation. In fact, this method has been applied to many physical systems showing strong non-Markovian effects (see, e. g., Refs. [6]–[8]).

In the present paper we apply the TCL projection operator technique to the model of a central spin interacting with a bath of N spins defined by the Hamiltonian ($\hbar=1$)

$$H = \frac{\omega_0}{2}\sigma_3 + \sum_{k=1}^{N} \alpha_k \boldsymbol{\sigma} \cdot \boldsymbol{\sigma}^k. \tag{1}$$

The Pauli operators $\boldsymbol{\sigma}$ and $\boldsymbol{\sigma}^k$ act on the Hilbert spaces of the central spin, which is regarded as the open quantum system, and of the k-th bath spin, respectively. The strength of the spin-bath coupling is given by the constants α_k. Moreover we have included an external magnetic field that acts on the central spin and leads to the Zeeman splitting ω_0.

The model given by the Hamiltonian [Eq. (1)] may be used to describe for example a single, localized electron spin coupled to a bath of nuclear spins in a quantum dot through contact hyperfine interaction.[9] It features many interesting phenomena such as nonexponential behavior of correlations and coherences and strong non-Markovian effects. A detailed treatment of the model within the NZ projection operator technique has been carried out in Ref. [10], and nonperturbative solutions for polarized initial conditions have been constructed in Ref. [11]. Recently, a detailed analytical and numerical study of the exact Bethe ansatz solution[12] of the

model has been carried out.[13] Moreover, several efficient numerical algorithms have been proposed that are based, e. g., on the spin-coherent-state representation[14] or on the Chebyshev expansion for the full propagator.[15]

The TCL projection operator method has been applied to various spin bath models for which a compact analytical solution is available, such as central spin models with Heisenberg XY (Ref. [16]) and with full Heisenberg interaction[17] for uniform couplings, and central spin models with nonuniform Ising interaction.[18] The purpose of the present paper is a detailed investigation of the performance of the TCL technique for the nontrivial model given by Eq. (1) with nonuniform couplings. To this end, we will compare the results for the populations and the coherences of the central spin obtained from the TCL approach to numerical simulations of the full von Neumann equation of the model. It will be demonstrated that the method provides an efficient scheme, which is applicable in the perturbative regime of weak couplings, even for long interaction times.

The paper is organized as follows. Sec. II contains a brief account of the TCL projection operator technique and its application to the model given by the Hamiltonian [Eq. (1)], as well as the derivation of the master equation governing the dynamics of the reduced density matrix of the central spin. We compare in Sec. III the solutions of this master equation to numerical simulations of the von Neumann equation corresponding to the Hamiltonian [Eq. (1)]. In Sec. IV we discuss the performance of an alternative TCL approach that is based on a modified interaction picture and leads to a simplified master equation. Finally, we draw our conclusions in Sec. V.

II. TCL MASTER EQUATION

A. Interaction picture

It is convenient to write the Hamiltonian [Eq. (1)] as $H = H_0 + H_I$, where

$$H_0 = \frac{\omega_0}{2}\sigma_3 + 2\sigma_3 K_3 \tag{2}$$

represents the unperturbed part, and

$$H_I = 2(\sigma_+ K_- + \sigma_- K_+) \qquad (3)$$

is the interaction Hamiltonian.[10] In Eq. (3) $\sigma_\pm$ are the raising and lowering operators of the central spin, whereas

$$K_3 = \frac{1}{2}\sum_{k=1}^{N} \alpha_k \sigma_3^k, \quad K_\pm = \sum_{k=1}^{N} \alpha_k \sigma_\pm^k. \qquad (4)$$

In the interaction picture defined by H_0 the interaction Hamiltonian becomes

$$H_I(t) = \sigma_+ B_-(t) + \sigma_- B_+(t), \qquad (5)$$

where

$$B_\pm(t) = 2e^{\mp i\omega_0 t}e^{\mp 2iK_3 t}K_\pm e^{\mp 2iK_3 t}. \qquad (6)$$

Thus the dynamics of the total system's density matrix $\rho(t)$ is governed by the von Neumann equation

$$\frac{d}{dt}\rho(t) = -i[H_I(t),\rho(t)] \equiv \mathcal{L}(t)\rho(t), \qquad (7)$$

where $\mathcal{L}(t)$ denotes the Liouville superoperator corresponding to the interaction Hamiltonian $H_I(t)$.

B. TCL projection operator approach

The starting point of the projection operator technique is the introduction of a suitable projection superoperator $\mathcal{P}$. This is a positive and trace-preserving linear map that acts on the operators of the total system with the property of a projection operator, i.e.. $\mathcal{P}^2 = \mathcal{P}$. The superoperator $\mathcal{P}$ is used to project any state ρ of the total system onto its relevant part $\mathcal{P}\rho$, expressing formally the elimination of the irrelevant degrees of freedom from the full dynamical description of the underlying model.[2]

Projection operator techniques are used to derive a closed equation of motion for the relevant part $\mathcal{P}\rho$. A special variant of these techniques is the TCL projection operator method. Given an initial state $\rho(0)$ satisfying $\mathcal{P}\rho(0) = \rho(0)$, this technique leads to a time-local first-order master equation for the relevant part of the form

$$\frac{d}{dt}\mathcal{P}\rho(t) = \mathcal{K}(t)\mathcal{P}\rho(t). \qquad (8)$$

Here, $\mathcal{K}(t)$ is a certain superoperator, representing the explicitly time-dependent generator of the quantum master equation for $\mathcal{P}\rho$. We note that, like the corresponding NZ equation, the TCL master [Eq. (8)] describes all non-Markovian effects although it is local in time.

In practical applications the TCL generator $\mathcal{K}(t)$ is mostly obtained from a perturbation expansion with respect to the strength of the interaction Hamiltonian,

$$\mathcal{K}(t) = \mathcal{K}_1(t) + \mathcal{K}_2(t) + \dots . \qquad (9)$$

The first-order contribution is given by

$$\mathcal{K}_1(t) = \mathcal{P}\mathcal{L}(t)\mathcal{P}, \qquad (10)$$

while the second-order term takes the form

$$\mathcal{K}_2(t) = \int_0^t dt_1 [\mathcal{P}\mathcal{L}(t)\mathcal{L}(t_1)\mathcal{P} - \mathcal{P}\mathcal{L}(t)\mathcal{P}\mathcal{L}(t_1)\mathcal{P}]. \qquad (11)$$

We remark that this expansion corresponds to an expansion in terms of the ordered cumulants of the Liouville operator[2] $\mathcal{L}(t)$.

In the present paper we restrict ourselves to the second order and employ the following projection superoperator:

$$\mathcal{P}\rho = \sum_m \mathrm{Tr}_B\{\Pi_m\rho\} \otimes \frac{1}{N_m}\Pi_m. \qquad (12)$$

Here, Tr_B denotes the partial trace over the spin bath, and the Π_m are ordinary projection operators acting in the conventional sense on the Hilbert space of the spin bath. They project onto the eigenspaces of the 3-component of the bath angular momentum,

$$J_3 = \frac{1}{2}\sum_{k=1}^{N} \sigma_3^k, \qquad (13)$$

corresponding to the eigenvalues $m = -N/2, \dots, N/2$. The quantity

$$N_m = \mathrm{Tr}_B \Pi_m = \binom{N}{\frac{N}{2}+m} \qquad (14)$$

represents the degree of degeneracy of the eigenvalue m of J_3. Explicitly, we have

$$\Pi_m = \sum_{\Sigma m^k = m} |m^1, m^2, \dots, m^N\rangle\langle m^1, m^2, \dots, m^N|, \qquad (15)$$

where $m^k = \pm\frac{1}{2}$ denotes the eigenvalue of the k-th bath spin operator $\frac{1}{2}\sigma_3^k$. Obviously, the projection operators Π_m fulfill the relations

$$\Pi_m \Pi_{m'} = \delta_{mm'}\Pi_{m'}, \quad \sum_m \Pi_m = I. \qquad (16)$$

With the help of Eq. (16) it is easy to verify that the projection superoperator [Eq. (12)] is indeed a completely positive and trace-preserving map that satisfies[19] $\mathcal{P}^2 = \mathcal{P}$. It projects a given state ρ onto a separable quantum state $\mathcal{P}\rho$, which describes classical correlations between the (unnormalized) system states

$$\rho_m(t) \equiv \mathrm{Tr}_B\{\Pi_m\rho(t)\} \qquad (17)$$

and the bath states Π_m/N_m. The latter represent states of maximal entropy under the constraint of a given value m for the total angular momentum. Finally, the reduced density matrix of the central spin is given by

$$\rho_S(t) = \mathrm{Tr}_B \rho(t) = \sum_m \rho_m(t). \qquad (18)$$

Thus, the dynamics of the central spin is determined by the dynamical variables $\rho_m(t)$, $m = -N/2, \dots, N/2$.

As mentioned already the TCL master [Eq. (8)] presupposes that the total system's initial state $\rho(0)$ fulfills the condition

$$\mathcal{P}\rho(0) = \rho(0). \tag{19}$$

If this condition is not satisfied one has to add a certain inhomogeneity to the right-hand side of the TCL master equation, which involves the initial conditions through the complementary projection $\mathcal{Q}\rho(0) = (I - \mathcal{P})\rho(0)$. In the standard applications of the projection operator techniques one employs a projection superoperator that projects onto an uncorrelated tensor product state. Condition (19) then holds, of course, if and only if the initial state is an uncorrelated state of the form $\rho(0) = \rho_S \otimes \rho_B$, where ρ_S is a state of the system and ρ_B is a state of the bath. However, the projection given by Eq. (12) belongs to the class of *correlated* projection superoperators,[8,19] which projects a given state ρ onto a correlated system-bath state. For this correlated projection condition (19) is satisfied if and only if the initial state is of the form

$$\rho(0) = \sum_m \rho_m(0) \otimes \frac{1}{N_m}\Pi_m. \tag{20}$$

Hence, the initial state may contain certain statistical correlations. A great advantage of the correlated projection operator technique is therefore given by the fact that it allows the treatment of correlated initial states by means of a homogeneous TCL master equation.

C. Deriving the master equation

For the interaction Hamiltonian [Eq. (5)] the projection operator [Eq. (12)] satisfies $\mathcal{P}\mathcal{L}(t)\mathcal{P} = 0$. Hence, to second order the TCL master Eq. (8) reduces to

$$\frac{d}{dt}\mathcal{P}\rho(t) = \int_0^t dt_1 \mathcal{P}\mathcal{L}(t)\mathcal{L}(t_1)\mathcal{P}\rho(t). \tag{21}$$

Taking into account the definition of $\mathcal{P}$ as given by Eq. (12) and exploiting the properties [Eq. (16)], it is possible to convince oneself that Eq. (21) is equivalent to the following system of coupled differential equations in the dynamical variables $\rho_m(t)$:

$$\frac{d}{dt}\rho_m(t) = -\sum_{m'} \int_0^t dt_1 \text{Tr}_B\left\{\Pi_m\left[H_I(t), \left[H_I(t_1), \rho_{m'}(t)\right.\right.\right.$$
$$\left.\left.\left. \otimes \frac{1}{N_{m'}}\Pi_{m'}\right]\right]\right\}.$$

Evaluating the double commutator we finally get the master equation

$$\frac{d}{dt}\rho_m(t) = \int_0^t d\tau\{[g_{m+1}(\tau) + g_{m+1}^*(\tau)]\sigma_+\rho_{m+1}(t)\sigma_-$$
$$+ [f_{m-1}(\tau) + f_{m-1}^*(\tau)]\sigma_-\rho_{m-1}(t)\sigma_+ - f_m(\tau)\sigma_+\sigma_-\rho_m(t)$$
$$- f_m^*(\tau)\rho_m(t)\sigma_+\sigma_- - g_m(\tau)\sigma_-\sigma_+\rho_m(t)$$
$$- g_m^*(\tau)\rho_m(t)\sigma_-\sigma_+\}. \tag{22}$$

The correlation functions $f_m(\tau)$ and $g_m(\tau)$ are defined by

$$f_m(\tau) = \langle B_-(t)B_+(t_1)\rangle_m, \tag{23}$$

$$g_m(\tau) = \langle B_+(t)B_-(t_1)\rangle_m, \tag{24}$$

with $\tau = t - t_1$ and

$$\langle\mathcal{O}\rangle_m = \frac{1}{N_m}\text{Tr}_B\{\mathcal{O}\Pi_m\}. \tag{25}$$

Exploiting Eq. (6) we find

$$f_m(\tau) = 4\sum_k \alpha_k^2 \langle\sigma_-^k\sigma_+^k e^{i(\omega_0 + 4K_3 + 2\alpha_k)\tau}\rangle_m, \tag{26}$$

$$g_m(\tau) = 4\sum_k \alpha_k^2 \langle\sigma_+^k\sigma_-^k e^{i(-\omega_0 - 4K_3 + 2\alpha_k)\tau}\rangle_m. \tag{27}$$

III. COMPARISON TO NUMERICAL SIMULATIONS

In this section we compare the dynamics of the density matrix $\rho_S(t)$ of the central spin obtained by solving the master Eq. (22) to the one deduced directly from the von Neumann Eq. (7). In particular we will consider the dynamics of both the coherences and the populations of the central spin starting from a fixed initial condition. To this end, we have carried out numerical simulations of the full von Neumann equation with mixed initial states for systems with up to $N = 10$ bath spins. Of course, the number of bath spins for which a direct numerical simulation of the von Neumann equation is possible is limited by the exponential increase in the dimension of the underlying Hilbert space. We note that the dimension of the total state space (the space of density matrices) is given by $D = 2^{2N+2} - 1$, which yields $D \approx 4 \cdot 10^6$ for $N = 10$.

In the following we assume that the hyperfine coupling constants are given by

$$\alpha_k = \alpha_0 \exp\left[-\left(\frac{k}{k_0}\right)^{n/d}\right], \tag{28}$$

where $k_0 = N/2$. We choose $n/d = 2$ corresponding to a Gaussian electronic wave function ($n = 2$) in one dimension ($d = 1$), which is of relevance in the context of a quantum dot.[10,13] We denote by A_1 the mean of the coupling constants α_k and by A_2 the respective root mean square,

$$A_1 = \frac{1}{N}\sum_k \alpha_k, \quad A_2 = \sqrt{\frac{1}{N}\sum_k \alpha_k^2}. \tag{29}$$

The initial state of the total system is taken to be $\rho(0) = \rho_S(0) \otimes \rho_B(0)$, where $\rho_B(0) = 2^{-N}I$ represents an unpolarized infinite temperature state (I denotes the unit matrix of the spin bath). With this initial state we have $\rho_m(0) = 2^{-N}N_m\rho_S(0)$. We emphasize that the present technique also allows the treatment of polarized and of correlated initial states (see Sec. II B).

A. Coherences

The coherence of the central spin is defined by $\widetilde{C}(t) = \langle + |\rho_S(t)| - \rangle$, where $|\pm\rangle$ denote the eigenstates of σ_3. According to Eq. (18) we have
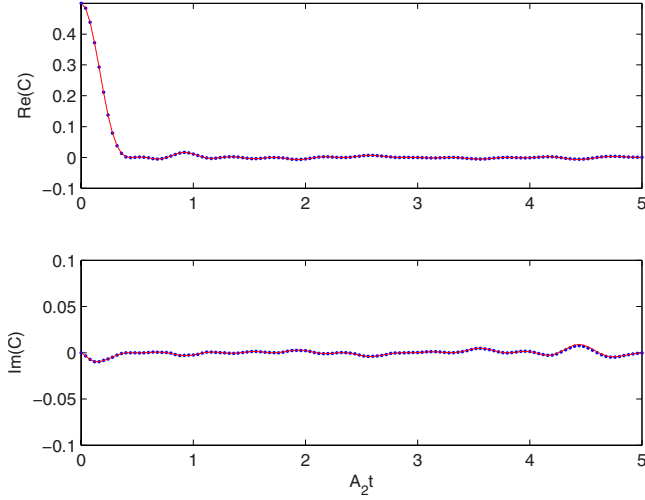
FIG. 1. (Color online) Real and imaginary parts of the coherence of the central spin for $\alpha_0/\omega_0 = 0.01$ and $N=10$ bath spins. Blue dots: Numerical simulation. Red line: TCL approximation according to Eq. (34).

$$\widetilde{C}(t) = \sum_m \widetilde{C}_m(t) = \sum_m \langle + |\rho_m(t)| - \rangle. \quad (30)$$

Starting from the master Eq. (22) we have

$$\frac{d}{dt}\widetilde{C}_m(t) = -\int_0^t d\tau [f_m(\tau) + g_m^*(\tau)]\widetilde{C}_m(t) \quad (31)$$

with the obvious solution

$$\widetilde{C}_m(t) = \widetilde{C}_m(0)e^{-\Lambda_m^{\rm coh}(t)}, \quad (32)$$

where

$$\Lambda_m^{\rm coh}(t) = \int_0^t dt_1 \int_0^{t_1} dt_2 [f_m(t_2) + g_m^*(t_2)]. \quad (33)$$

Let's now remember that the master equation [Eq. (22)] has been written in the interaction picture with respect to the Hamiltonian [Eq. (2)]. As usual, we will represent our results in the interaction picture with respect to the free Hamiltonian $(\omega_0/2)\sigma_3$, which is in the rotating frame of the central spin. In order to do this we have to use the replacement

$$\sum_m \rho_m(t) \otimes \frac{\Pi_m}{N_m} \rightarrow \sum_m e^{-2i\sigma_3 K_3 t}\rho_m(t) \otimes \frac{\Pi_m}{N_m} e^{2i\sigma_3 K_3 t}.$$

It is immediate to observe that under this transformation the populations remain unchanged, while the coherences must be multiplied by the factor $\langle e^{-4iK_3 t}\rangle_m$. Hence, the coherence $C(t)$ in the rotating frame of the central spin is found to be

$$C(t) = C(0)\sum_m \frac{N_m}{2^N}\langle e^{-4iK_3 t}\rangle_m e^{-\Lambda_m^{\rm coh}(t)}. \quad (34)$$

In Fig. 1 we compare the result of the TCL approximation given by Eq. (34) to numerical simulations of the von Neumann Eq. (7) supposing that the central system is initially prepared in the superposition state $\frac{1}{\sqrt{2}}(|+\rangle + |-\rangle)$. Correlation

functions (26) and (27), and the mean value $\langle e^{-4iK_3 t}\rangle_m$ have been calculated numerically. As it is evident from the figures the agreement between the TCL result and the numerical solution is excellent in the perturbation regime, even for long integration times.

B. Populations

The populations $P_\pm(t) = \langle \pm |\rho_S(t)| \pm \rangle$ of the central spin are given by

$$P_\pm(t) = \sum_m P_m^\pm(t) = \sum_m \langle \pm |\rho_m(t)| \pm \rangle. \quad (35)$$

The master equation [Eq. (22)] leads to a system of coupled equations,

$$\frac{d}{dt}P_m^+(t) = \int_0^t d\tau [g_{m+1}(\tau) + g_{m+1}^*(\tau)]P_{m+1}^-(t) - [f_m(\tau) + f_m^*(\tau)]P_m^+(t), \quad (36)$$

$$\frac{d}{dt}P_m^-(t) = \int_0^t d\tau [f_{m-1}(\tau) + f_{m-1}^*(\tau)]P_{m-1}^+(t) - [g_m(\tau) + g_m^*(\tau)]P_m^-(t). \quad (37)$$

To solve these equations we employ the relation

$$\frac{d}{dt}[P_m^+(t) + P_{m+1}^-(t)] = 0, \quad (38)$$

which expresses the conservation of the 3-component of the total spin angular momentum. Using the initial condition $P_+(0)=1$ we obtain

$$P_+(t) = \sum_m \frac{N_m}{2^N}e^{-\Lambda_m^{\rm pop}(t)}\left[1 + \int_0^t dt_1 e^{\Lambda_m^{\rm pop}(t_1)}\mu_m(t_1)\right], \quad (39)$$

where

$$\Lambda_m^{\rm pop}(t) = 2\,{\rm Re}\int_0^t dt_1 \int_0^{t_1} dt_2 [g_{m+1}(t_2) + f_m(t_2)], \quad (40)$$

and

$$\mu_m(t) = 2\,{\rm Re}\int_0^t d\tau g_{m+1}(\tau). \quad (41)$$

The comparison of the TCL result [Eq. (39)] with the numerical simulation is shown in Fig. 2. We again observe a very good agreement of the TCL approximation with the exact dynamics for short and also for long interaction times. Due to the exponential increase in the numerical effort with increasing N we can treat only a relatively small number of bath spins. Thus we have an open quantum system, the central spin, which is coupled to a relatively small environment, a finite system of bath spins. For this reason, the conventional techniques used in the theory of open systems to derive a Markovian master equation are not applicable because they are usually based on an effectively infinite environment with a continuum of bath modes. However, the TCL approxi-
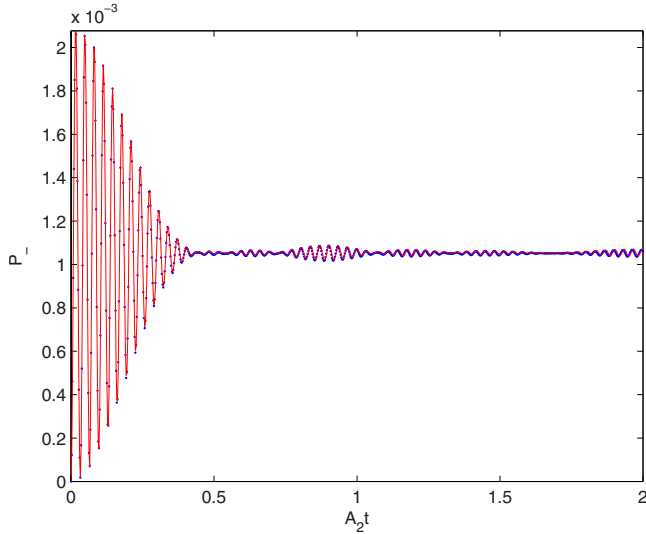
FIG. 2. (Color online) Population of the central spin for $\alpha_0/\omega_0=0.01$ and $N=10$ bath spins. Blue dots: Numerical simulation. Red line: TCL approximation according to Eq. (39).

mation scheme developed here does not require that N be large. The master Eq. (22) is therefore valid also for a very small number of bath spins. We illustrate this point in Figs. 3 and 4, which show the dynamics of the coherences and the populations for $N=6$ bath spins.

The master equation [Eq. (22)] has been obtained from the second order of the TCL perturbation expansion. Of course, for much stronger system-bath couplings the second-order result fails, indicating the relevance of cumulants of higher order. To illustrate this point we have increased α_0 by a factor of ten. The result for the coherences and the populations is depicted in Figs. 5 and 6, respectively. We observe that the short-time behavior is still correctly reproduced by the second order, while there are large deviations for longer times. We conclude from our numerical simulations that the
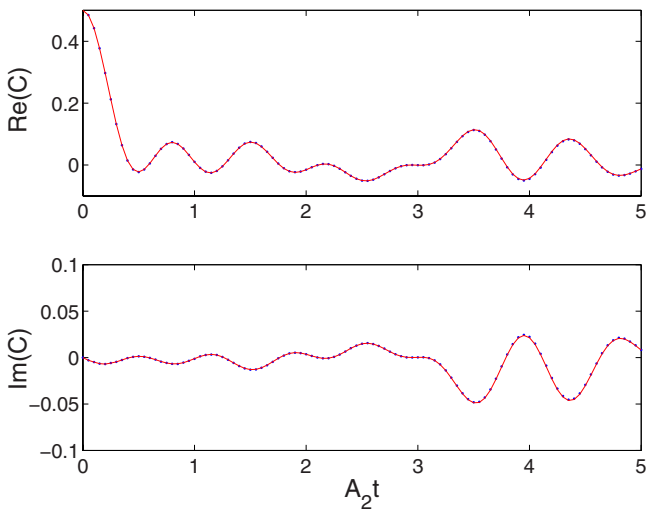

FIG. 3. (Color online) Real and imaginary parts of the coherence of the central spin for $\alpha_0/\omega_0=0.01$ and $N=6$ bath spins. Blue dots: Numerical simulation. Red line: TCL approximation according to Eq. (34).
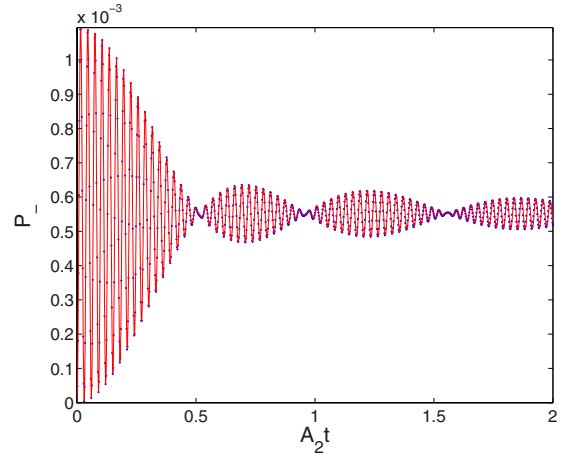

FIG. 4. (Color online) Population of the central spin for $\alpha_0/\omega_0=0.01$ and $N=6$ bath spins. Blue dots: Numerical simulation. Red line: TCL approximation according to Eq. (39).

second order of the TCL scheme yields a good agreement with the exact dynamics for couplings up to the order of $\alpha_0/\omega_0 \sim 10^{-2}$. Note however that the decay of the coherence $C(t)$ and the corresponding decoherence time are very well reproduced even for much larger couplings as can be seen from Figs. 5.

IV. MODIFIED INTERACTION PICTURE

A certain disadvantage of the perturbation scheme used in Sec. II consists in the fact that the time integrals over the correlations functions in Eqs. (33) and (39)–(41) are generally difficult to calculate and have to be determined numerically. To avoid the appearance of these expressions and to obtain a simpler approximation scheme we employ a modification of the interaction picture Hamiltonian. To this end, we write the Hamiltonian [Eq. (1)] again as $H=H_0+H_I$, where now the unperturbed part is given by
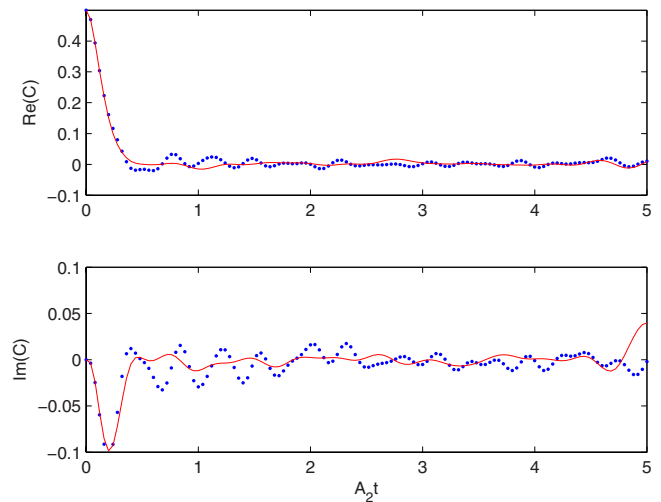

FIG. 5. (Color online) Real and imaginary parts of the coherence of the central spin for $\alpha_0/\omega_0=0.1$ and $N=10$ bath spins. Blue dots: Numerical simulation. Red line: TCL approximation according to Eq. (34).
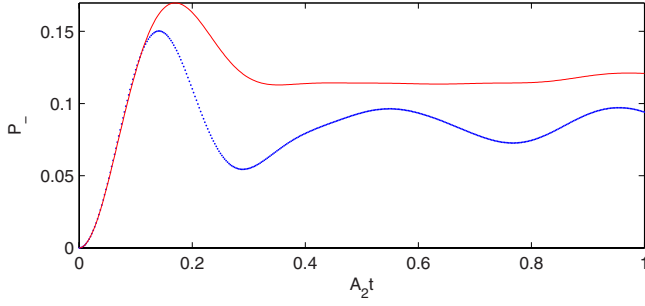
FIG. 6. (Color online) Population of the central spin for $\alpha_0/\omega_0 = 0.1$ and $N = 10$ bath spins. Blue dots: Numerical simulation. Red line: TCL approximation according to Eq. (39).

$$H_0 = \frac{\omega_0}{2}\sigma_3 + 2A_2\sigma_3 J_3, \qquad (42)$$

and

$$H_I = 2\sigma_3(K_3 - A_2 J_3) + 2(\sigma_+ K_- + \sigma_- K_+) \qquad (43)$$

represents the interaction Hamiltonian. By contrast to the interaction picture of Sec. II, here the diagonal term $2\sigma_3 K_3$ of the Hamiltonian [Eq. (1)] is not completely removed from the interaction, but we subtract only the term $2A_2\sigma_3 J_3$ involving an effective coupling constant A_2 that is equal to the root mean square of the α_k [see Eqs. (13) and (29)]. Hence, the interaction picture Hamiltonian now takes the form

$$H_I(t) = 2\sigma_3(K_3 - A_2 J_3) + \sigma_+ B_-(t) + \sigma_- B_+(t), \qquad (44)$$

where

$$B_\pm(t) = 2e^{\mp i\omega_0 t}e^{\mp 2iA_2 J_3 t}K_\pm e^{\pm 2iA_2 J_3 t}. \qquad (45)$$

The corresponding Liouville operator will again be denoted by $\mathcal{L}(t)$.

An important point of the new interaction picture is that for Hamiltonian (44) and projection (12) the first-order term $\mathcal{P}\mathcal{L}(t)\mathcal{P}$ does not vanish. Hence, one has to use the full expressions Eqs. (10) and (11) for the second-order TCL generator. However, the great advantage of the present procedure is the fact that the correlation functions Eqs. (23) and (24) take on a very simple form

$$f_m(\tau) = B_+(m)e^{i\Omega_+(m)\tau}, \qquad (46)$$

$$g_m(\tau) = B_-(m)e^{i\Omega_-(m)\tau}, \qquad (47)$$

where

$$\Omega_\pm(m) = \pm\omega_0 + 4A_2\left(\pm m + \frac{1}{2}\right)$$

and

$$B_\pm(m) = 4A_2^2\left(\frac{N}{2} \mp m\right).$$

With the help of these expressions we find the master equation

$$\frac{d}{dt}\rho_m(t) = 2im(A_2 - A_1)[\sigma_3, \rho_m(t)] - \frac{N^2 - 4m^2}{N-1}$$

$$\times (A_2^2 - A_1^2)t[\sigma_3, [\sigma_3, \rho_m(t)]] + \int_0^t d\tau$$

$$\times \{B_-(m+1)2\cos[\Omega_+(m)\tau]\sigma_+\rho_{m+1}(t)\sigma_-$$

$$+ B_+(m-1)2\cos[\Omega_-(m)\tau]\sigma_-\rho_{m-1}(t)\sigma_+$$

$$- B_+(m)e^{i\Omega_+(m)\tau}\sigma_+\sigma_-\rho_m(t)$$

$$- B_+(m)e^{-i\Omega_+(m)\tau}\rho_m(t)\sigma_+\sigma_-$$

$$- B_-(m)e^{i\Omega_-(m)\tau}\sigma_-\sigma_+\rho_m(t)$$

$$- B_-(m)e^{-i\Omega_-(m)\tau}\rho_m(t)\sigma_-\sigma_+\}. \qquad (48)$$

In the special case of uniform couplings ($\alpha_k = $const) we have $A_1 = A_2$. Equation (48) then reduces to the master equation derived in Ref. 17.

The master equation [Eq. (48)] can again be solved analytically. The procedure is similar to the one outlined in Sec. II. We find the coherences,

$$C(t) = C(0)\sum_m \frac{N_m}{2^N}e^{-\Lambda_m^{\text{coh}}(t)}, \qquad (49)$$

where

$$\Lambda_m^{\text{coh}}(t) = 4iA_1 mt + 2\frac{N^2 - 4m^2}{N-1}(A_2^2 - A_1^2)t^2 + \frac{B_+(m)}{\Omega_+^2(m)}$$

$$\times [1 - e^{i\Omega_+(m)t}] + \frac{B_-(m)}{\Omega_-^2(m)}[1 - e^{-i\Omega_-(m)t}]$$

$$+ it\left[\frac{B_+(m)}{\Omega_+(m)} - \frac{B_-(m)}{\Omega_-(m)}\right], \qquad (50)$$

and the populations,

$$P_+(t) = \sum_m \frac{N_m}{2^N}\left[\frac{\frac{N}{2}+m+1}{N+1} + \frac{\frac{N}{2}-m}{N+1}e^{-\Lambda_m^{\text{pop}}(t)}\right], \qquad (51)$$

where

$$\Lambda_m^{\text{pop}}(t) = \frac{8A_2^2(N+1)}{\Omega_+^2(m)}(1 - \cos[\Omega_+(m)t]). \qquad (52)$$

Involving only a sum over the quantum number m, expressions (49) and (51) can be evaluated numerically in a very efficient way. The comparison to the numerical simulation of the von Neumann equation demonstrates that also the TCL approach with the modified interaction picture yields a good agreement. The decoherence (see Fig. 7), as well as the oscillations and the decay of the populations (see Fig. 8), is very well reproduced by the simplified scheme. For longer interaction times the result [Eq. (51)] leads to revivals of the populations (see Fig. 9), which are due to the commensurability of the frequencies $\Omega_+(m)$. We stress that these revivals are neither present in the exact solution nor in the TCL approximation [Eq. (39)]. Apart from these revivals the simplified approximation given by the master equation [Eq. (48)]
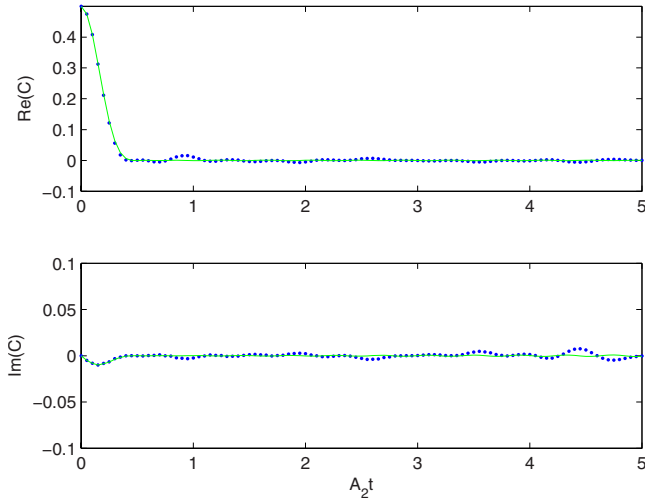
FIG. 7. (Color online) Real and imaginary parts of the coherence of the central spin for $\alpha_0/\omega_0 = 0.01$ and $N = 10$. Blue dots: numerical simulation. Green line: TCL approximation according to Eq. (49).

thus provides an accurate description of the decoherence and of the oscillating decay of the populations.

Finally we investigate the limit of a large number N of bath spins. For small values of the quantity $\beta \equiv 2\sqrt{N}A_2/\omega_0$ and large N the result [Eq. (51)] can be approximated by

$$P_+(t) \approx 1 - \beta^2[1 - e^{-2NA_2^2 t^2} \cos \omega_0 t]. \tag{53}$$

To obtain this expression one first expands the exponential in Eq. (51) for small Λ_m^{pop} and carries out the summation over m. Equation (53) provides a good approximation for a fixed $\beta \ll 1$ even for moderate N values. For example, the case of $N = 10$ bath spins with $\alpha_0/\omega_0 = 0.01$ investigated above corresponds to $\beta = 0.03$. For this value of β, we find that Eq. (53) yields a good agreement for all N larger than about 10.
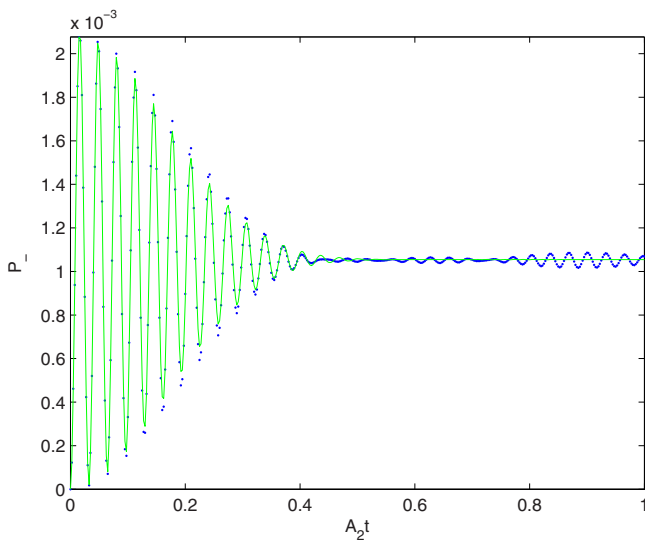

FIG. 8. (Color online) Population of the central spin for $\alpha_0/\omega_0 = 0.01$ and $N = 10$. Blue dots: Numerical simulation. Green line: TCL approximation according to Eq. (51).
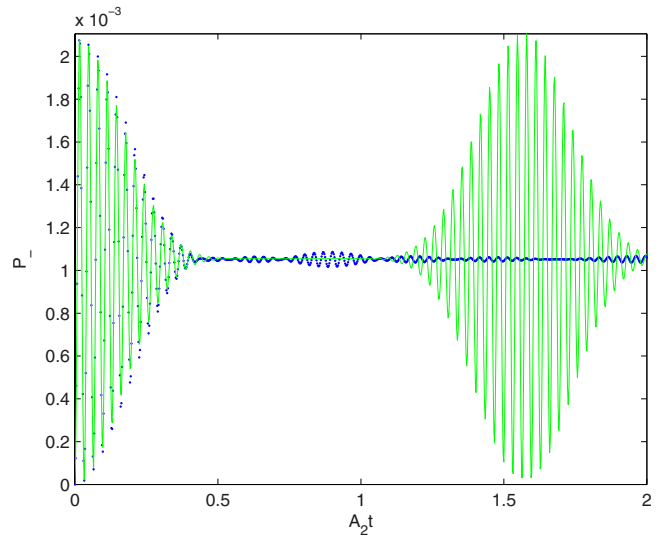

FIG. 9. (Color online) The same as Fig. 8 for a longer interaction time.

V. CONCLUSIONS

The appearance of a retarded memory kernel in the equations of motion, e.g., in the Nakajima-Zwanzig equation, is often regarded as *the* characteristic feature of non-Markovian quantum processes. However, applications of the time-convolutionless projection operator technique show that strong non-Markovian behavior of open quantum systems can often be described by time-local master equations with an explicitly time-dependent generator. Although there is no theory of non-Markovian dynamics which allows a general assessment of the NZ and the time-convolutionless (TCL) scheme, experience shows that in many physical systems the degree of accuracy achieved by both methods is of the same order of magnitude. In such cases the TCL method is clearly to be preferred because it only requires solving a time-local master equation. This does not mean that the TCL technique is always better than the NZ technique. The performance of these perturbation schemes strongly depends on the details of the system under investigation and on the chosen projection superoperator. There are examples of physical systems for which either the NZ or the TCL approach yields the exact result already in lowest order of perturbation theory.[17,20]

In the present paper we have demonstrated the feasibility of the TCL approach in the case of a nontrivial model describing a central spin coupled to a spin bath through non-uniform Heisenberg interaction. We have shown that the method indeed works in the strong field limit and provides a good approximation of the short and the long-time behavior of the coherences and the populations of the central spin. In addition, we have developed a TCL master equation that is based on a modified interaction picture and leads to a compact analytical solution for the central spin's density matrix, which allows an efficient numerical computation.

A possible approach to moderate or strong couplings is the analysis of the ordered cumulants of higher orders in the TCL expansion. However, it seems that a more efficient strategy consists in the construction of more suitable correlated projection superoperators. An example of this strategy

is discussed in Ref. 17, where a certain correlated projection has been constructed for which the second-order Nakajima-Zwanzig master equation leads to the exact dynamics of the population for the Hamiltonian [Eq. (1)] with uniform couplings. It is of great relevance to develop possible extensions of this strategy to the nonuniform spin bath model analyzed here.

*ferraro@fisica.unipa.it

†breuer@physik.uni-freiburg.de

[1] R. Kubo, M. Toda, and N. Hashitsume, *Statistical Physics II. Nonequilibrium Statistical Mechanics* (Springer, Berlin, 1991).

[2] H.-P. Breuer and F. Petruccione, *The Theory of Open Quantum Systems* (Oxford University Press, Oxford, 2007).

[3] S. Nakajima, Prog. Theor. Phys. **20**, 948 (1958).

[4] R. Zwanzig, J. Chem. Phys. **33**, 1338 (1960).

[5] S. Chaturvedi and F. Shibata, Z. Phys. B **35**, 297 (1979).

[6] H. P. Breuer, B. Kappler, and F. Petruccione, Ann. Phys. (N.Y.) **291**, 36 (2001).

[7] D. Ahn, J. Lee, M. S. Kim, and S. W. Hwang, Phys. Rev. A **66**, 012302 (2002).

[8] H. P. Breuer, J. Gemmer, and M. Michel, Phys. Rev. E **73**, 016139 (2006).

[9] J. Schliemann, A. Khaetskii, and D. Loss, J. Phys.: Condens. Matter **15**, R1809 (2003).

[10] W. A. Coish and D. Loss, Phys. Rev. B **70**, 195340 (2004).

[11] A. V. Khaetskii, D. Loss, and L. Glazman, Phys. Rev. Lett. **88**, 186802 (2002).

[12] M. Gaudin, J. Phys. (France) **37**, 1087 (1976).

[13] M. Bortz and J. Stolze, Phys. Rev. B **76**, 014304 (2007).

[14] K. A. Al-Hassanieh, V. V. Dobrovitski, E. Dagotto, and B. N. Harmon, Phys. Rev. Lett. **97**, 037204 (2006).

[15] V. V. Dobrovitski and H. A. De Raedt, Phys. Rev. E **67**, 056702 (2003).

[16] H. P. Breuer, D. Burgarth, and F. Petruccione, Phys. Rev. B **70**, 045323 (2004).

[17] J. Fischer and H. P. Breuer, Phys. Rev. A **76**, 052119 (2007).

[18] H. Krovi, O. Oreshkov, M. Ryazanov, and D. A. Lidar, Phys. Rev. A **76**, 052117 (2007).

[19] H.-P. Breuer, Phys. Rev. A **75**, 022103 (2007).

[20] R. Steinigeweg, H.-P. Breuer, and J. Gemmer, Phys. Rev. Lett. **99**, 150601 (2007).